Polaron States in a CuO Chain

K. Bieniasz[a,*] and A.M. Oleś[a,b]

[a]Marian Smoluchowski Institute of Physics, Jagiellonian University, W.S. Reymonta 4, PL-30-059, Kraków, Poland
[b]Max-Planck-Institut für Festkörperforschung, Heisenbergstr. 1, D-70569 Stuttgart, Germany

We introduce a one-dimensional model for a CuO chain, with holes and $S = 1/2$ spins localized in $3d_{x^2-y^2}$ orbitals, and p_σ oxygen orbitals without holes in the ground state. We consider a single hole doped at an oxygen site and study its propagation by spin-flip processes. We develop the Green function method and treat the hole-spin coupling in the self-consistent Born approximation, similar to that successfully used to study polarons in the regular t–J model. We present an analytical solution of the problem and investigate whether the numerical integration is a good approximation to this solution.

1. Introduction

Soon after the discovery of high-T_c superconductors (HTS), it was realized that the t–J model could be regarded as the prime candidate for the theoretical description of the phenomenon [1]. A deeper insight into the dynamics of a hole propagation in a Mott insulator with antiferromagnetic (AF) order might yield a clue to the understanding of the origin of superconductivity in cuprates [2]. The effective t–J model arises from mapping the three-band p–d model [3, 4] onto the copper $d_{x^2-y^2}$ states and provides the simplest description of the electronic states in CuO_2 planes of HTS. Recent studies indicate, however, that oxygen p-orbital states strongly renormalize the quasiparticle (QP) energy, both for antiferromagnetic [5] and ferromagnetic [6] systems. Importance of oxygen orbitals may be recognized both from the prominent role played in cuprates by the second neighbor effective hopping t', for instance in the stability of stripe phases [7], and from numerical studies comparing hole-doped and electron-doped systems [8].

These circumstances have led us to study the polaron dynamics in the extended t–J model which includes the oxygen states. In analogy to the well known CuO_2 system, initially the $2p$ oxygen states are completely filled with electrons, while the $d_{x^2-y^2}$ states are half-filled and hosting localized $S = 1/2$ spins. The superexchange J couples the spins on Cu sites [9] and stabilizes AF order in the ground state. In the charge-transfer insulator there are no itinerant charges in the p states. Therefore, to activate any kinetic energy or interaction whatsoever, one needs to inject charges into the p states, which is usually achieved by means of hole doping $La_{2-x}(Sr,Ca)_xCuO_4$, or by substitutional transition metal impurities of different valence than Cu ions. Here we consider the case of a single hole injected into the p-band.

The complexity of hopping processes in a realistic CuO_3 chain in $YBa_2Cu_3O_7$ [10] motivates a simpler one-dimensional (1D) model of a CuO chain, see Fig. 1. The advantage of this linear structure is that interoxygen hopping is avoided and one may focus on the hole dynamics of a carrier injected into one of the oxygen orbitals, which follows from three-site processes, as shown below. Such processes are of crucial importance in systems where other hopping processes cannot occur, as in t_{2g} systems with Ising-like superexchange, where they cause weak hole propagation [11] and stabilize bond stripes [12], and in the quantum compass model [13].
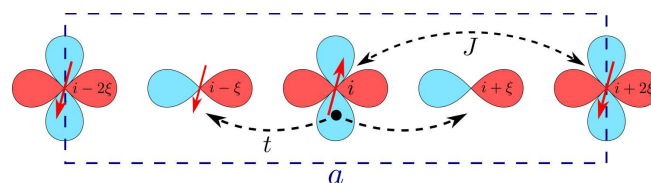

Fig. 1. Schematic representation of the CuO model with the conventions used throughout this paper. The dashed line frame indicates the magnetic unit cell in real space. Spins at Cu sites interact by the AF superexchange J, and t stands for the spin-flip p–d–p three-site hopping.

2. Model

We formulate the simplest 1D t–J-like model with hole dynamics in p orbitals. The model Hamiltonian,

$$\mathcal{H} = \mathcal{H}_0 + \mathcal{V}, \tag{1}$$

consists of magnetic Heisenberg exchange (2a), enforcing the AF ground state in the "Cu" d states and a three-site p–d–p spin-flip hopping (2b), obtained in second order perturbation theory, acting as the interaction

$$\mathcal{H}_0 = J\sum_i (\boldsymbol{S}_i \cdot \boldsymbol{S}_{i+2\xi} - S^2), \tag{2a}$$

$$\mathcal{V} = t\sum_{i,\sigma} (p^\dagger_{i+\xi,\bar\sigma} d_{i\bar\sigma} d^\dagger_{i\sigma} p_{i-\xi,\sigma} + \text{H.c.}), \tag{2b}$$

where $\xi = a/4$, a is the magnetic unit cell length, the

*corresponding author; e-mail:
krzysztof.bieniasz@uj.edu.pl

constants J (superexchange) and t (hopping) are defined as positive, and the summation extends over all the crystal unit cells. The model follows in perturbation theory from the respective itinerant model for the CuO chain. Note that this simple Hamiltonian does not include any free electron kinetic terms which are blocked due to large Coulomb repulsion on $d_{x^2-y^2}$ orbitals, and therefore the free electrons are dispersionless. For a graphic illustration of the model and the various conventions pertaining to it, consult Fig. 1.

To solve this toy model in the self-consistent Born approximation (SCBA) [14], one should first notice that the pairs of fermion operators at Cu sites are equivalent to spin-flip processes,

$$d_{i\bar{\sigma}}d_{i\sigma}^{\dagger} = -S_i^{\sigma}, \tag{3}$$

where the right hand side is the spin raising/lowering operator, depending on the value of the spin index σ. SCBA is typically employed using the linear spin wave (LSW) theory, where one expands the spin operators in powers of bosonic operators up to the second order using the Holstein–Primakoff representation. All the calculations are done here in the magnetic unit cell, as the expansion of (2b) around the AF ground state is irreducible to the crystal unit cell.

After performing the standard steps of Fourier and Bogoliubov transformations in the two sublattice framework, one arrives at the following representation of the Hamiltonian (2):

$$\mathcal{H}_0 = \sum_q \omega_q(\alpha_q^{\dagger}\alpha_q + \beta_q^{\dagger}\beta_q), \tag{4a}$$

$$\mathcal{V} = \frac{4t}{\sqrt{N}}\sum_{kq}\Gamma_{kq}\left[p_{k+q,\uparrow}^{\dagger}p_{k\downarrow}(\alpha_{-q}^{\dagger} + \beta_q) + \text{H.c.}\right], \tag{4b}$$

where $\omega_q = J|\sin(q/2)|$ is the magnon dispersion relation in the 1D AF model (2a), N is the number of magnetic unit cells in the system, and

$$\Gamma_{kq} = \sin\frac{k+q}{4}\sin\frac{k}{4}(u_q + v_q) \tag{5}$$

is the electron–magnon vertex function. The operators $\{\alpha_q, \beta_q\}$ are the bosonic Bogoliubov operators and $\{u_q, v_q\}$ are the Bogoliubov transformation coefficients. More details on the above derivation can be found in the literature concerning polarons in the t–J model, particularly in [14].

To obtain the SCBA Green function solution, one needs to calculate the self-energy, which then serves as the basis for the first order Green function

$$\Sigma(k,\omega) = \langle 0|p_{k\sigma}\mathcal{V}\mathcal{G}(\omega)\mathcal{V}p_{k\sigma}^{\dagger}|0\rangle, \tag{6}$$

$$\mathcal{G}(\omega) = [\omega + i\eta - \mathcal{H}]^{-1}, \tag{7}$$

where $|0\rangle$ is the AF ground state and $\mathcal{G}(\omega)$ is the resolvent, or the Green function operator. Note that, because of the spin degrees of freedom, $\Sigma(k,\omega)$ is in fact a 2×2 matrix, although only in a trivial, diagonal manner. Inserting (4) into (6) one quickly arrives at the following expression for the first order self-energy:

$$\Sigma^{(1)}(k,\omega) = \frac{16t^2}{N}\sum_{q\in\text{BZ}}\frac{\Gamma_{kq}^2}{\omega - \omega_q}\mathbb{I}_2, \tag{8}$$

where $\mathbb{I}_2$ is a 2×2 identity matrix to account for the aforementioned spin degrees of freedom and the summation extends over the first Brillouin zone (BZ). The above equation can be solved analytically for the present 1D case, yielding

$$\Sigma^{(1)}(k,\omega) = \frac{2}{\omega}\cos^2\frac{k}{4}\left(\frac{1}{\sqrt{1-\omega^2}}\ln\frac{\sqrt{1-\omega^2}-1}{\omega} + \ln\frac{2\omega-2}{\omega}\right)$$
$$+ \cos\frac{k}{2}\left(\frac{\pi}{2} - \frac{\omega}{\sqrt{1-\omega^2}}\ln\frac{\sqrt{1-\omega^2}-1}{\omega}\right), \tag{9}$$

as we will show elsewhere since the details of this derivation are beyond the scope of this article.

On the other hand, the self-energy (8) can also be calculated numerically by simple lattice summation over the BZ. After this is accomplished, $\Sigma^{(1)}(k,\omega)$ can be used to obtain the first order Green function via the equation

$$G(k,\omega) = [(\omega + i\eta)\mathbb{I}_2 - \Sigma(k,\omega)]^{-1}, \tag{10}$$

which forms the basis of the self-consistent solution. Equation (10) can then be inserted into (6) to obtain the second order self-energy, and so on. However, usually the first order solution suffices and further iterations do not change the result significantly. Indeed, this is also the case here (not shown). Once the Green function is calculated, one can extract the physical information in the form of the spectral function

$$A(k,\omega) = -\frac{1}{2\pi}\Im[\text{Tr}G(k,\omega)], \tag{11}$$

which has a direct relation to photoelectron spectroscopy experiments.

3. Results and discussion

Here we will present the numerical results (for self-energy in the first order) obtained by the method described above, and contrast them against the first order analytic result, as mentioned earlier. As can be seen from (8), the natural unit of energy for this problem is the parameter J, therefore the results are plotted using the energy ω/J.

Figure 2 shows the density map of the numerically obtained spectral function $A(k,\omega)$ (in gray-scale) for the problem under consideration with $t = 1$. Bear in mind that in order to expose the low-amplitude features of the spectrum, a nonlinear tanh-scale has been employed, hence the very strong "broadening" of the bands.

On top of the numerical result we have plotted the analytic solution (solid red line). This plot was obtained by solving the equation

$$\omega - \Re[\Sigma^{(1)}(k,\omega + i\eta)] = 0, \tag{12}$$

which defines the location of the QP bands, sans the broadening of the spectrum, i.e., the resulting curve corresponds to the QP maxima of (11). Next we will discuss the differences between the two results.

First of all, one notices that both the numerical and the analytic results display two solution branches: (i) the lower branch with negative energy which is a bound QP state (since the reference free particle dispersion is 0), and (ii) the upper branch, which is an excited
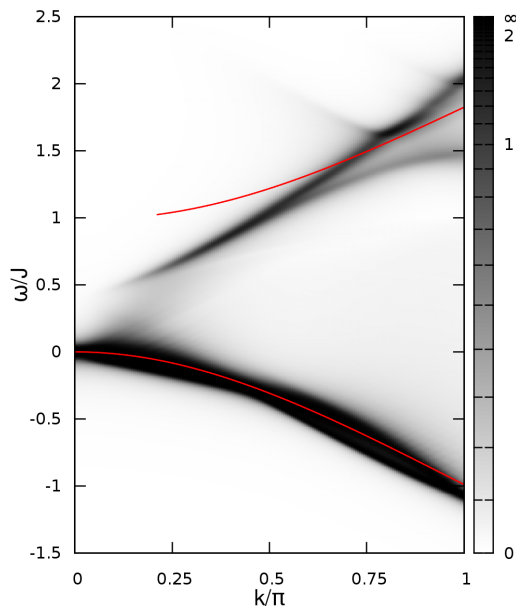
Fig. 2. Numerically calculated spectral function $A(k,\omega)$ (gray scale) and the analytic solution (solid red lines) for $t = 1$ and $\eta = 0.01$. Note the nonlinear tanh-scale.

QP state — in the present case, as the analytic result seems to suggest, it exists only for $k \gtrsim \pi/4$.

It is evident from Fig. 2 that in the case of the lower branch the analytic result reproduces the numerical solution quite well in the whole range of k values. On the other hand, one can easily notice a sharp discrepancy between the two results in the case of the upper branch. While the analytic result ends rather abruptly around the energy $\omega/J = 1$, the numerical solution extends well below this point. Since the analytic solution does not employ any approximations (beyond the physical ones), we rather expect the numerical approach to be unsound.

It is our supposition that the problem lies within the too naive approach to the numerical integration. More specifically, the function being integrated in (8) is proportional to $(\omega - |\sin(q/2)|)^{-1}$, which has a singularity line in the range $\omega \in [0, 1]$. Integrating such a function numerically using simple quadrature rules, such as the rectangle rule in this case, introduces noticeable systematic errors into the solution. Such errors should be especially visible in the range in which the divergence occurs. As can be seen in Fig. 2, this is indeed the case since the discrepancy between the two solutions is most pronounced exactly in the range where the singularities occur.

Further, from (8) one can see that in order to calculate $\Sigma(k,\omega)$, one needs to integrate all the $(k-q, \omega - \omega_q)$ elements, which means that the errors introduced in the lower energies propagate to the solution at higher energies, which would explain the mismatch between the solutions also for $\omega > J$. Moreover, this implies that a naive numerical solution of the problem presented herein is reliable only until the energy $\omega \approx 0$.

4. Summary

In summary, we have presented the exact analytic result and an approximate numerical solution of the formulated problem of the hole motion along the CuO chain generated by spin-flip processes. By comparing them we have emphasized that an unsophisticated approach to numerical methods can be detrimental to the reliability of the SCBA results.

Acknowledgments

References

[1] M. Ogata, H. Fukuyama, *Rep. Prog. Phys.* **71**, 036501 (2008).

[2] A.M. Oleś, *Acta Phys. Pol. A* **121**, 752 (2012).

[3] C.M. Varma, S. Schmitt-Rink, E. Abrahams, *Solid State Commun.* **62**, 681 (1987).

[4] A.M. Oleś, J. Zaanen, P. Fulde, *Physica B+C* **148**, 260 (1987).

[5] B. Lau, M. Berciu, G.A. Sawatzky, *Phys. Rev. Lett.* **106**, 036401 (2011).

[6] K. Bieniasz, A.M. Oleś, *Phys. Rev. B* **88**, 115132 (2013); *Acta Phys. Pol. A* **126**, A80 (2014).

[7] M. Fleck, A.I. Lichtenstein, A.M. Oleś, *Phys. Rev. B* **64**, 134528 (2001).

[8] E. Arrigoni, M. Aichhorn, M. Daghofer, W. Hanke, *New J. Phys.* **11**, 055066 (2009).

[9] J. Zaanen, A.M. Oleś, *Phys. Rev. B* **37**, 9423 (1988).

[10] A.M. Oleś, W. Grzelka, *Phys. Rev. B* **44**, 9531 (1991).

[11] M. Daghofer, K. Wohlfeld, A.M. Oleś, E. Arrigoni, P. Horsch, *Phys. Rev. Lett.* **100**, 066403 (2008).

[12] P. Wróbel, A.M. Oleś, *Phys. Rev. Lett.* **104**, 206401 (2010).

[13] W. Brzezicki, M. Daghofer, A.M. Oleś, *Phys. Rev. B* **89**, 024417 (2014); *Acta Phys. Pol. A* **127**, 263 (2014).

[14] G. Martínez, P. Horsch, *Phys. Rev. B* **44**, 317 (1991).